An Investigation into the Effects of a Transient *Kdm5c* Deletion in Imprinted X Chromosome Inactivation

By
Reina Brodeur

An honors thesis submitted in partial fulfillment
of the requirements for graduation with honors in the degree of
Biological Physics
at the University of Michigan

April 2023

Sponsors:
Sundeep Kalantry, PhD
Professor, Department of Human Genetics
University of Michigan Medical School

Michal Zochowski, PhD
Professor of Biophysics and Physics, Department of Biophysics
University of Michigan

Table of Contents

Abstract

As mammalian X and Y chromosomes evolved from autosomes, they slowly lost the ability to recombine with each other. As a result, there has been a gradual loss of Y linked genes overtime. To equalize sex linked gene expression between male and females, mammals evolved X-chromosome inactivation (XCI), a mechanism by which one of two X chromosomes is silenced during female embryogenesis through the use of the long non-coding (lnc)RNA Xist.

Since X and Y chromosomes evolved from regularly recombining autosomes, they share a set of homologous genes, many of which escape inactivation on the X chromosome. One such X linked gene, *Kdm5c,* which encodes for the histone demethylase enzyme KDM5C, has been shown to upregulate *Xist* expression in therian mammal epiblast cells. Ectopic expression of this gene induced Xist RNA in ~15-20% of male mouse embryonic stem cells (mESCs). Further study of *Kdm5c* gene expression in epiblast-like cells (EpiLCs) found that the loss of the KDM5C enzyme in mutant cells reduced Xist RNA expression significantly when compared to non-mutant lines. Xist RNA expression in EpiLCs and ESCs therefore appears to be dosage dependent on KDM5C levels. My research focuses on the effects that mutated *Kdm5c* gene expression has on *Xist* induction and regulation in extraembryonic endoderm (XEN) and trophoblast stem (TS) cells using biophysical methods such as RT-qPCR and RNA Fluorescent in Situ Hybridization (FISH).

Introduction

X Chromosome Inactivation (XCI)

X chromosome inactivation (XCI) is a method of dosage compensation that equalizes sex linked gene expression between male and female therian mammals. This became an evolutionary necessity as mammalian sex chromosomes evolved, due to the lack of genetic recombination between the X and Y chromosomes, and in turn the gradual loss of Y-linked genes overtime. During early embryogenesis, the X-inactive specific transcript (*Xist*) gene, which encodes for a long non-coding (lnc)RNA, is upregulated on the soon to be silenced X chromosome. Once upregulated, Xist forms an RNA coating in *cis* around the X chromosome, effectively blocking transcriptional factors, thus silencing it. Studies have shown that increased *Xist* expression is necessary for the initiation of X inactivation. Xist RNA additionally recruits other cofactors which together create and preserve histone modifications that maintain X inactivation during further embryonic development.

In mice, two forms of XCI occur (Figure 1). First, during the two cell stage of female embryogenesis, all cells in the zygote initiate imprinted X inactivation, where exclusively the paternally inherited X chromosome (X_p) is silenced. As the blastocyst develops, cells that will differentiate into the embryo proper lose the epigenetic markers that maintain X_p silencing, reactivating this chromosome. It is important to note that extraembryonic tissues maintain their imprinted X inactivation at this stage and throughout later development. During the late blastocyst stage, cells of the inner cell mass begin to initiate random X inactivation, where each cell arbitrarily silences either

the maternally inherited chromosome (X_m) or the X_p. After this, X inactivation is stably maintained in extraembryonic tissues and the embryo.

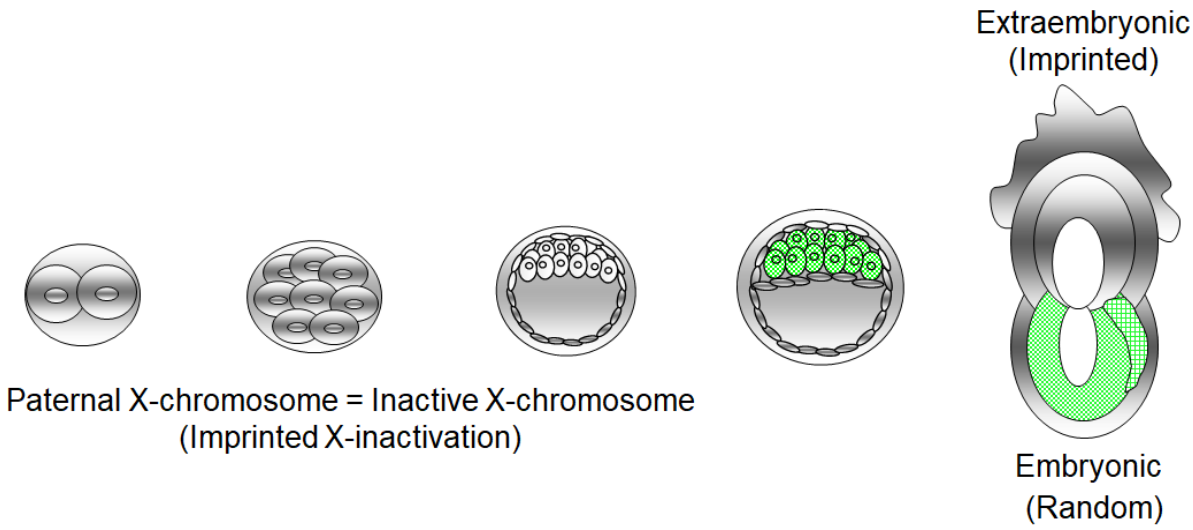

Figure 1: Depiction of imprinted and random X inactivation for 2 cell, 8 cell, early blastocyst, late blastocyst, and post-implantation stages of mouse embryo development.

XY Homologous Genes

Despite differentiating from each other nearly 100 million years ago, some genes that remain on the Y chromosome still have a homologous gene present on the X chromosome. It is interesting to note that these X linked homologs almost invariably escape XCI, and are still expressed on the female inactive X chromosome (X_i). One possible reason for this, is that a dosage compensation method is not necessary for these homologs as the X copy and the Y copy could serve the same function. Whether an individual is XY or XX, they will still receive and express two copies of these traits and therefore do not need to be silenced on the X chromosome.

However, these homologs have had ~100 million years to evolve independently of each other. Since the X and Y chromosomes are so disparate, no genetic recombination can occur between them, meaning sex linked genes often maintain non-lethal amino acid substitutions. As a result, XY homologs could be functionally distinct from one another. If that is the case, then these genes may escape X inactivation because they evolved a female-specific role. The theory that we explore here hypothesizes that these genes escape X inactivation because they play some role in inducing and/or stabilizing XCI in mammalian females.

Role of *Kdm5c in XCI*

One homologous gene pair, X linked gene *Kdm5c* and its Y linked homolog *Kdm5d,* encode the enzyme Lysine Demethylase 5C (KDM5C) and 5D (KDM5D), respectively. Both KDM5C and KDM5D demethylate the histone H3 di- and tri-methylated lysine 4 (H3K4me2 and H3K4me3) modifications, transforming them into H3 mono-methylated lysine (H3K4me1), a marker associated with gene enhancers. Because *Kdm5c* escapes X inactivation, our lab decided to investigate if *Kdm5c* plays a role in *Xist* induction by studying how Xist RNA levels change in response to altered *Kdm5c* expression.

Previous research has shown that *Xist* activators are expressed at a higher level in female derived cell lines than male derived ones. When our lab tested *Kdm5c* gene expression in wildtype mouse epiblast stem cells (EpiSCs) and embryonic stem cells (ESCs), this trend continued, as *Kdm5c* RNA levels were significantly higher in female derived lines than male lines, consistent with this gene having a possible role in *Xist*

induction. This same study conducted by our lab found that ectopically expressing *Kdm5c*, but not *Kdm5d*, in mouse ESCs resulted in increased Xist RNA expression in ~15-20% of XY male cell lines. These data show that *Kdm5c* has a dose-dependent function, separate from *Kdm5d*, in inducing Xist RNA expression. This further supports the theory that *Kdm5c* plays a female specific role in inducing XCI. The dose dependent role of *Kdm5c* in *Xist* expression was further tested using epiblast-like cells (EpiLCs) that were mutant for *Kdm5c*. This work from our lab showed that *Kdm5c* is necessary and sufficient to enhance Xist RNA expression in a dose-dependent manner: Namely that increased KDM5C increased Xist RNA levels, while mutant or enzymatically inactive KDM5C enzymes reduced Xist RNA levels.

The results above lend support to the theory that *Kdm5c* escapes X inactivation because of the female specific role it plays in initiating said process. Importantly though, this study only focused on cell lines derived from the inner cell mass. As stated above, these cells undergo random X inactivation where either the X_m or the X_p can be silenced. To expand upon this research, my project focuses on the role *Kdm5c* plays in initiating imprinted X inactivation.

Results

Previous research I conducted through this lab focused on studying the effects *Kdm5c* mutations had on imprinted X inactivation in mouse blastocysts. My work used microscopy and RNA fluorescent in situ hybridization (FISH) to quantify RNA levels in cell nuclei. *Kdm5c*$^{-/-}$ mouse blastocysts were stained and the number of Xist coats they expressed counted. These values were then compared to blastocysts that were *Kdm5c*$^{-/+}$ and *Kdm5c*$^{+/+}$ to see if *Kdm5c* expression had an impact on Xist RNA levels. We hypothesized that reducing levels of KDM5C in the embryos would reduce the number of nuclei showing Xist RNA coating of the inactive X chromosome, similar to the results found by our lab in ESCs and EpiLCs. When quantifying these data however, no significant changes in Xist RNA levels could be seen between the different groups. One possible reason for this is that the embryos were derived from *Kdm5c*$^{-/-}$ oocytes, so the deletion occurred too early in development. As a result, the embryo was able to adjust to the change in gene expression by compensating with other factors responsible for inducing X inactivation. This in turn leads to similar signals between the three genotypes by the embryo (E) day 3.5 stage (Figure 2).

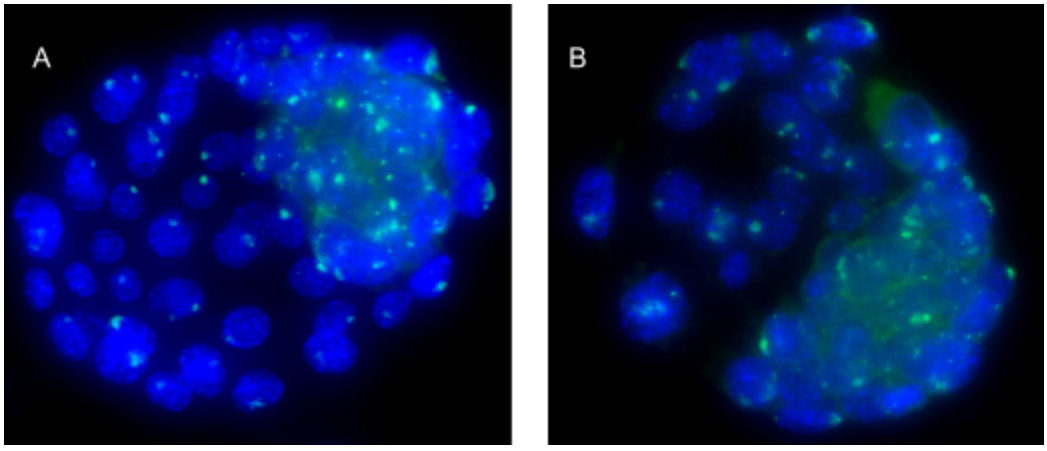

Figure 2: *Kdm5c*$^{-/+}$ (a) and *Kdm5c*$^{-/-}$ (b) E3.5 mouse blastocysts. Cell nuclei are represented by DAPI (blue). Xist RNA coats are represented by FITC (green pinpoints).

Because of this, we decided to focus instead on replicating this experiment in a cell culture model using a transient *Kdm5c* deletion. The use of a transient deletion in cell lines allows for precise time point collections that are not possible when working with blastocysts. This allows for data to be recorded mere hours after a deletion occurs. For my research, having these precise data points could allow us to see changes in Xist RNA levels before the cells are able to compensate for the change in *Kdm5c* gene expression. Since cell lines can adapt to environmental changes quickly, they can develop non-canonical methods of *Xist* expression and X inactivation not typically seen *in vivo*, in an attempt to survive in culture for as long as possible. By instead inducing a deletion and collecting results from early timepoints, we can study the immediate effects a *Kdm5c* deletion has on Xist RNA expression before a cell line has time to adapt to the change: thus recording data more reflective of the processes occuring *in vivo.*

Additionally, a major benefit to cell culture that embryos lack, is the amount of data that can be collected for relatively little work. For one, cell lines are much easier to derive and reproduce experiments in than embryos. They can be treated for RNA FISH, as well as collected for RNA extraction and real time quantitative polymerase chain reactions (RT-qPCRs): two techniques that rely quite heavily on biophysical methods to work.

My research this year focused on trophoblast stem (TS) cells and extraembryonic endoderm (XEN) cells that were *Kdm5c*$^{fl/fl}$ or *Kdm5c*$^{fl/y}$. Both of these cells are derived from the extraembryonic tissues in embryos which undergo imprinted XCI. The flox (fl)

allele of *Kdm5c* will phenotypically behave the same as a wild-type allele, but upon the addition of *Cre* recombinase the lox sites present in the gene will recombine, leading to the excision of the intermediate sequence, in this case the *Kdm5c* gene. These cell lines also carry an ERT2 *Cre* transgene. This form of *Cre* is induced when exposed to the drug Tamoxifen in high enough concentrations, creating the *Kdm5c* deletion. Using PCR and gel electrophoresis, derived TS and XEN cells were genotyped to ensure that all cell lines carried the *Kdm5c* flox alleles and the ERT2 *Cre* gene. Using this system, we are able to engineer transient *Kdm5c* mutations in cell lines by treating them with Tamoxifen. After a deletion occurs, Xist RNA expression is compared between treated and untreated cells to see the impact *Kdm5c* has on inducing *Xist*.

Since Tamoxifen is a powder that is reconstituted in 100% Ethanol, a drug toxic to cells in high concentrations, an initial test was conducted on TS and XEN cells to determine what concentration of Tamoxifen was necessary to ensure the deletion of *Kdm5c* without exposing cells to harmful levels of ethanol. A line of $Kdm5c^{+/+}$ cells were plated in six well plates and treated with Tamoxifen at 0, 3, 5, 7, 9 and 10 μM concentrations. These concentrations were picked based on previous research done in $Xist^{fl/+}$ TS cells which used a Tamoxifen concentration of 9μM. After treatment with Tamoxifen, the cell death and morphology for derived cell lines were compared to a control group which received no treatment to determine Tamoxifen toxicity.

Based on the results of the above experiment, a final concentration of 2.5 μM of Tamoxifen was decided upon. To confirm that the Tamoxifen was actually inducing ERT2 *Cre,* cells were treated with the drug over a time course of 0-3 days. Both TS and XEN cells were plated at ~70% confluency into four 24-well plates. One well received

media mixed with ethanol to act as a vehicle control while the others were treated with media containing tamoxifen. DNA lysates from the cells and media were collected from one well every 24 hours for 3 days. Media in the other wells was replaced every 24 hours and cells were retreated with either tamoxifen or ethanol. The media in the well was collected because it contained dead cells. This was one way to assess if cells with the *Kdm5c* deletion were dying and would not be present in the cell lysate. After collecting lysates from each time point, cells were genotyped to confirm a $Kdm5c^{fl/fl}$ to $Kdm5c^{-/-}$ mutation.

It is interesting to note that in TS cells, the tamoxifen treatment seemed to have no effect, even when the treatment dosages were increased to 5, 10 and 15 μM. We also tested multiple $Kdm5c^{fl/fl}$ cell lines to ensure that these results were not because of a spontaneous mutation in one cell line. A similar test in a line of $Eed^{fl/fl}$ TS cells, another gene proven to play a role in regulating X inactivation, also showed no signs of an *Eed* deletion occurring. Because of the lack of response to Tamoxifen treatment in TS cells, further research looking at these cells was halted. Instead, the Tamoxifen treatment must be optimized further before experiments can proceed. The rest of my research this semester focused only on inducing the transient deletion in XEN cells, which were receptive to the tamoxifen treatment at a 2.5 μM concentration (Figure 3).

After the Tamoxifen deletion was confirmed to work in two lines of XEN cells, a $Kdm5c^{fl/fl}$ and $Kdm5c^{fl/y}$ line, further experimentation could proceed. Cells from each XEN line were plated into two 6-well dishes to be treated in triplicate with either 2.5 μM Tamoxifen or an equivalent volume of 100% Ethanol (as a control) for 1 or 2 days.

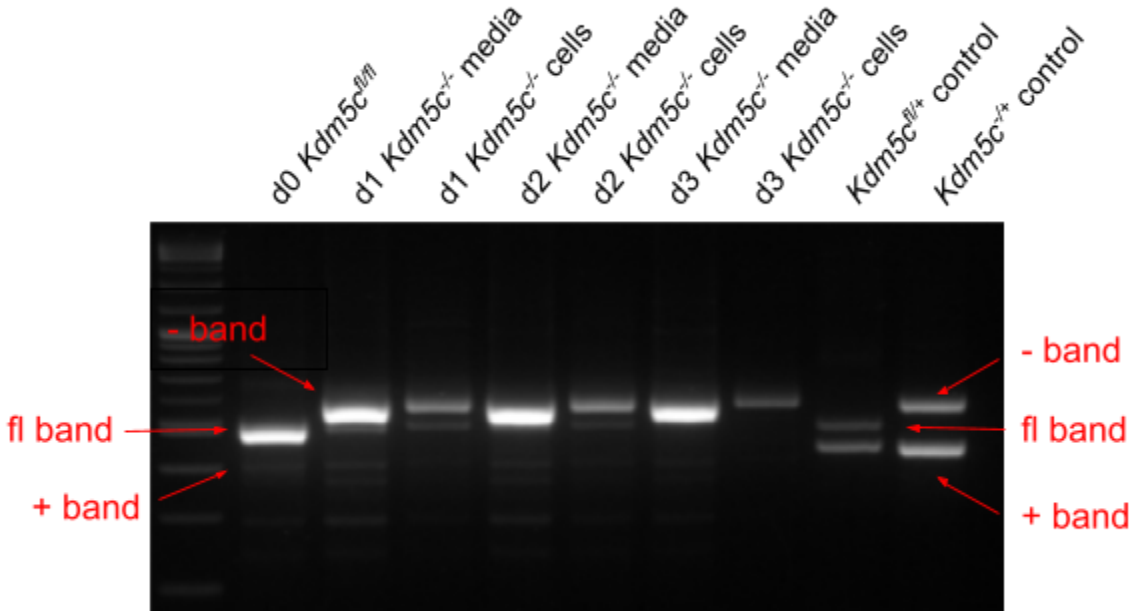

Figure 3: PCR results to confirm *Kdm5c*$^{fl/fl}$ transient deletion in XEN cell line for 0, 1, 2, and 3 days of treatment with Tamoxifen.

These cells were then treated in cytoskeletal buffer (CSK) and stained for RNA FISH microscopy. An additional 6-well dish was plated down to collect RNA lysates for 1, 2 and 3 days of either Tamoxifen or ethanol treatment to be used for RNA extractions and RT-qPCR.

RNA FISH staining is a biophysical technique that uses fluorescent probes that bind to specific nucleic acids to visualize gene expression in cells. This research method is especially important in genetics research where the majority of studies focus on changing gene expression. FISH can be used to confirm changes in DNA or RNA levels, it can be combined with immunofluorescence, and it can be used to stain both embryos or cells on a coverslip giving it a vast range of biological applications. The main physical principle used in FISH is fluorescent excitation and emission. First, a

fluorescent microscope illuminates the sample with light to excite the fluorophores in the FISH probe (Figure 4). Once excited, these fluorophores will relax to a lower energy level, releasing light of a longer wavelength as they do so. The emitted photons can be detected by the eye or a camera and quantified. Cells are stained with DAPI (a fluorescent dye which binds to DNA) to help visualize the nucleus, while the precipitated probe binds to specific mRNA transcripts; In this case Xist coats appear as green through the FITC microscope channel and Atrx pinpoints can be seen as red dots on the Cy3 microscope channel (Figure 2, Figure 5).

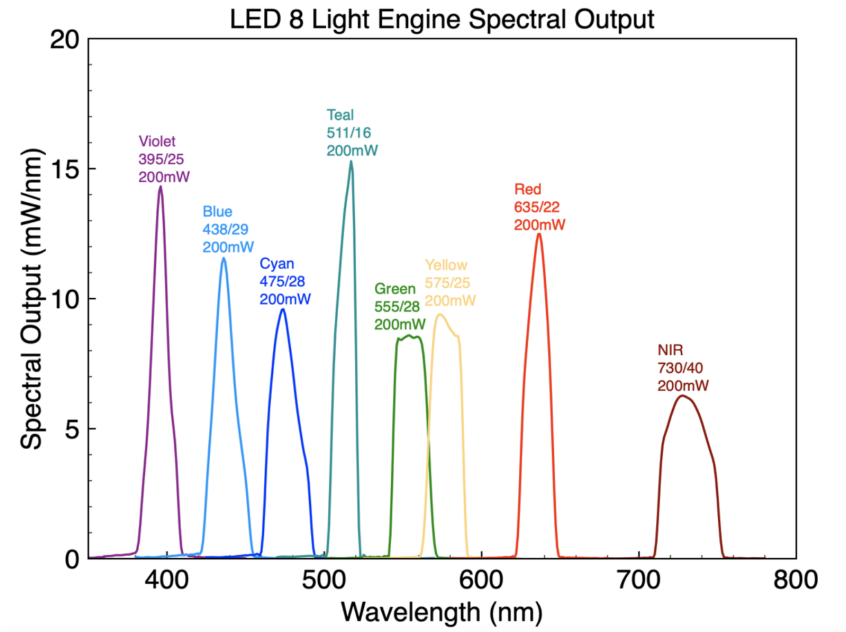

Figure 4: Spectral output of LED8 color spectrum. Different outputs can be used to excite fluorophores which can then be detected and quantified using the Leica Microscope camera

One potential area of study for this experiment uses a new Leica microscope containing the LED8 lightsource, with 8 possible outputs. This is an additional four spectrums that can be used compared to what the older Nikon microscope was capable of. The availability of these additional wavelengths of light will allow for more complex

experiments to be done and allow us to multiplex more genes with RNA FISH and also stain proteins localized to the inactive-X at the same time.

CSK treated cells were stained for RNA FISH and visualized using a Nikon Eclipse TiE inverted microscope (Figure 5). Similar to the results seen in the *Kdm5c* mutant embryos, after 2 days of Tamoxifen treatment, there was little to no change in Xist coat expression levels when compared to the ethanol treated controls. On both coverslips, Xist coats can be seen clearly in the nuclei surrounding the X_i. The red Atrx pinpoint can also be clearly seen in the nuclei which confirms the presence of a second, active X chromosome in these cells. The absence of an Atrx pinpoint overlapping with the Xist RNA coat confirms successful inactivation of the Xist-coated X chromosome.

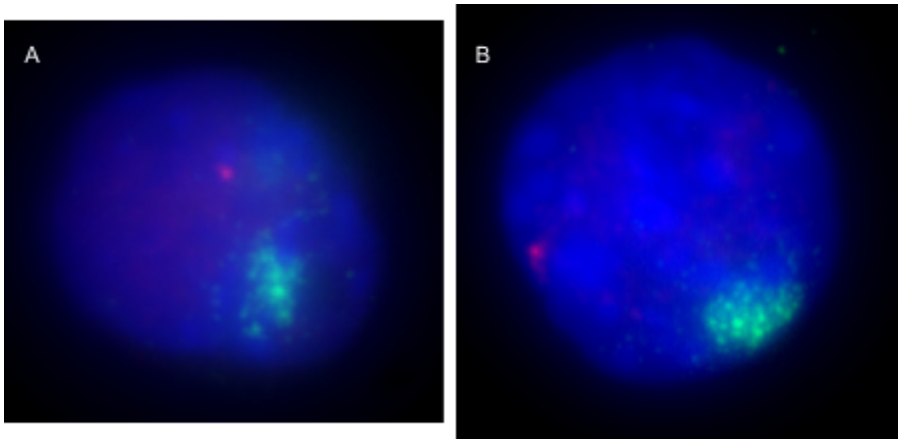

Figure 5: Day 2 treated Ethanol (a) and Tamoxifen (b) *Kdm5c*$^{-/-}$ cell nuclei stained with DAPI (blue). Xist RNA coats are represented by FITC (green pinpoints). Atrx RNA is represented by Cy3 (red pinpoints).

Cells plated down for RT-qPCR were collected and their RNA extracted. RT-qPCR is another powerful biophysical method, as it detects changes in a gene's RNA levels. During RT-qPCR, RNA extracted from the cell lysates is first reverse transcribed into complementary (c)DNA, then amplified using DNA polymerase. DNA

levels are measured during the amplification process by their fluorescent signal due to the presence of a fluorescent intercalating dye used to stained nucleotides. The level of DNA expression is then compared to a housekeeping gene, in this case *Tbp,* and CT values generated. As seen in Figure 6a below, *Kdm5c* was successfully deleted in XEN cells after one day of Tamoxifen treatment, and this deletion was maintained through days 2 and 3. This is to be expected since a *Kdm5c* deletion occurred within the first 24 hours of Tamoxifen treatment according to gel electrophoresis data. Relative Xist RNA levels on the other hand showed no significant change between the ethanol control groups and the Tamoxifen treatment groups (Figure 6b).

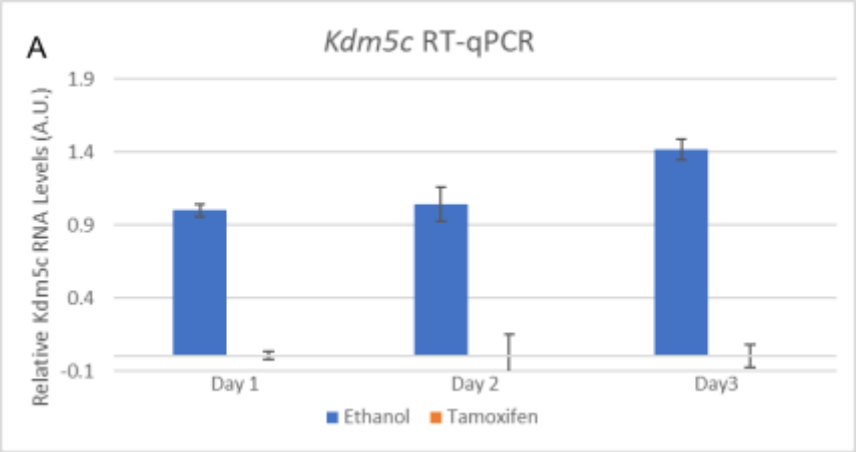

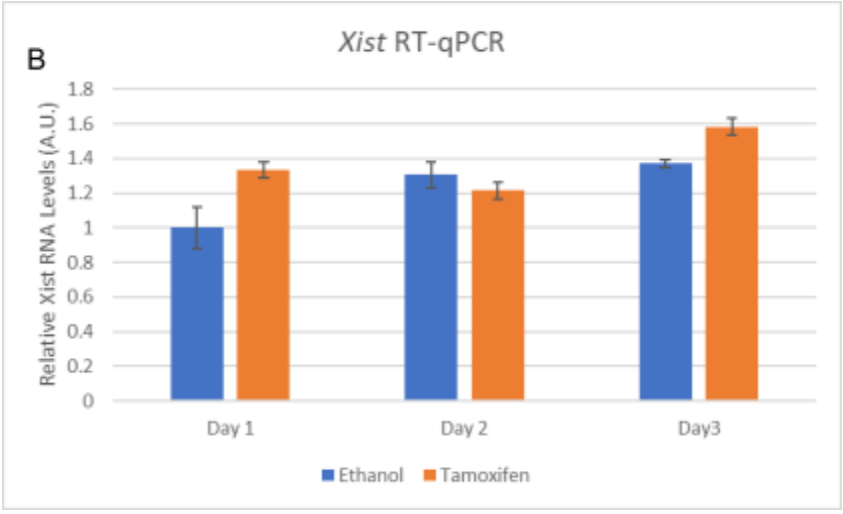

Figure 6: RT-qPCR for *Kdm5c* (a) and Xist (b) relative RNA levels

The results of both the RNA FISH and the RT-qPCR data are consistent with what was seen in the *Kdm5c* mutant embryos. One possible reason for this is the time course chosen for these cells was too long; The cells would have had enough time to adapt to the changed RNA levels and induce X inactivation by compensating with other mechanisms. Research I am currently conducting is focused instead on replicating these experiments for shorter time scales, using 8, 16 and 24 hours. DNA lysates have confirmed a transient *Kdm5c* deletion for these timepoints (Figure 7). Additionally, CSK treated coverslips for RNA FISH have already been made and RNA has been extracted for further RT-qPCR quantification.

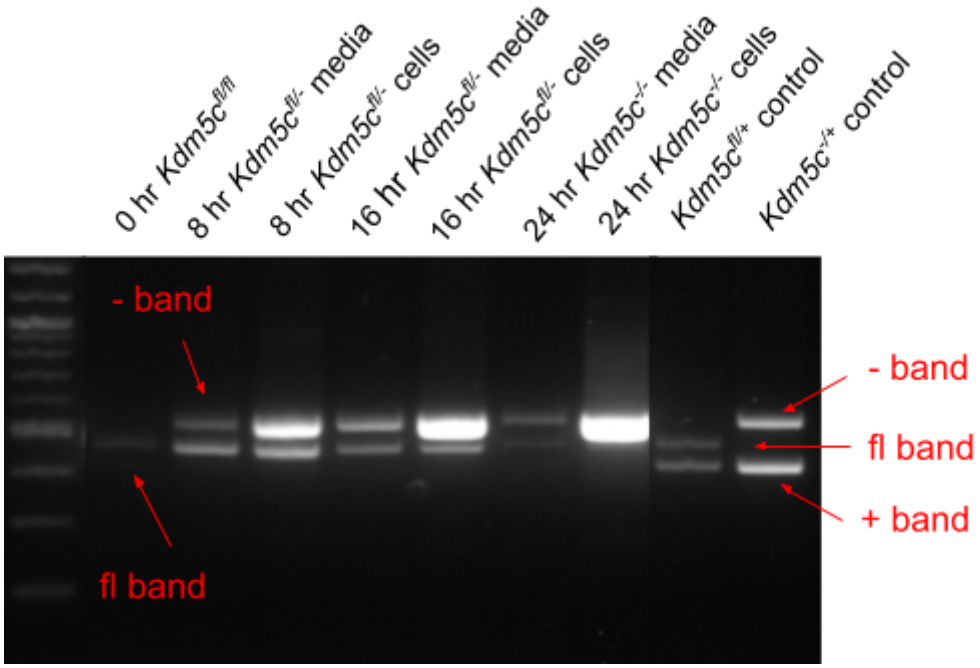

Figure 7: PCR results to confirm *Kdm5c*$^{fl/fl}$ transient deletion in XEN cell line for 8, 16 and 24 hrs of treatment with Tamoxifen.

Discussion

In this study I analyzed the effects a transient *Kdm5c* deletion has on Xist RNA levels in TS and XEN cells. Most of the experiments I have conducted thus far have focused on deriving cell lines and utilizing biophysical methods such as RT-qPCR and RNA FISH to study changes in gene expression and RNA levels. While some optimization must still be done, especially in TS cell lines which are not currently inducing a *Kdm5c* deletion when exposed to Tamoxifen, much of the groundwork has been laid for future studies.

As mentioned above, I am currently working on replicating these experiments for a shorter time course, using 8, 16 and 24 hr collection times instead of 1, 2 and 3 days. There is some promising data which indicates that this will be a more effective time course. Using PCR and gel electrophoresis, a *Kdm5c* deletion was shown to occur overtime for these collection times. As seen in Figure 7, the $Kdm5c^{fl}$ band begins to fade at the 8 hr mark before completely disappearing at the 24 hr mark. The 24 hr media DNA lysate sample shows some presence of the $Kdm5c^{fl}$ band in the gel likely due to the presence of dead cells found in the media that died before a deletion could be induced.

The gradual change in *Kdm5c* expression is the reason we wanted to induce a transient deletion with Tamoxifen. Our previous research in ESCs and EpiLCs indicates a dosage dependence of Xist RNA levels on *Kdm5c* gene expression where Xist RNA levels increased with ectopic *Kdm5c* expression, and were reduced when the enzyme KDM5C was enzymatically inactive. When replicating these experiments in embryos, TS and XEN cells, to look at the role *Kdm5c* plays specifically in inducing imprinted X

inactivation, we would expect to see similar results. Namely, that as *Kdm5c* is deleted in the cells, Xist RNA levels will slowly decrease. Most of our research so far has likely focused on a time scale too long to properly display this effect however. Cells and embryos are able to adapt to changes in gene expression, and can compensate for *Kdm5c* gene deletion with other biological processes responsible for inducing and maintaining X inactivation. We hope that with these new collection time points, it would be difficult for cells to adjust to the change in gene expression and adapt new methods of inducing Xist coats. Because of this, any RNA FISH staining and RT-qPCR data we collect will then be representative of processes *Kdm5c* induces *in vivo,* and further confirm that imprinted X inactivation is dose dependent on *Kdm5c*. This would also confirm the female specific role that *Kdm5c* plays in inducing imprinted X inactivation, and one potential explanation as to why this X homolog escapes XCI. The absence of a change in Xist RNA expression upon deletion of *Kdm5c* in XEN cells might suggest a different role of *Kdm5c* in imprinted vs random X-chromosome inactivation. As these processes are thought to work through similar mechanisms, this would be a significant finding worthy of further study.

Additionally, whether or not Xist RNA levels are depleted when a transient *Kdm5c* deletion is induced in TS and XEN cell lines, this study is still significant because it deepens our knowledge of X and Y linked homologs that escape X inactivation. Understanding the role these genes play in inducing X inactivation, both imprinted and random, helps us better understand the processes involved in gene induction, maintenance and silencing in the human genome.

Methods

Ethics Statement

This study was performed in strict accordance with the recommendations in the Guide for the Care and Use of Laboratory Animals of the National Institutes of Health. All animals were handled according to the protocols approved by the University Committee on Use and Care of Animals (UCUCA) at the University of Michigan (protocol #PRO00006455 and PRO00010233).

Embryo Dissections and Processing.

Pre-implantation embryonic (E) day 3.5 embryos were flushed from the uterine limbs in 1X PBS (Invitrogen, #14200075) containing 6 mg/mL bovine serum albumin (BSA; Invitrogen, #15260037). For fluorescence *in situ* hybridization (FISH) staining of embryos, the zona pellucida surrounding E3.5 embryos were removed through incubation in cold Acidic Tyrode's Solution (Sigma, #T1788), followed by neutralization through several transfers of cold M2 medium (Sigma, #M7167). Isolated embryos were plated onto gelatin-coated glass coverslips in 0.25X PBS with 6 mg/mL BSA for RNA (FISH) staining. For plated embryos, excess solution was aspirated, and coverslips were air-dried for 15 min. After drying, embryos were permeabilized and fixed in 50 mL solution of 0.05% Tergitol (Sigma, #NP407) and 1% paraformaldehyde (Electron Microscopy Sciences, #15710) in 1X PBS for 10 min. Excess solution was tapped off onto paper towels, and coverslips were rinsed 3X with 70% ethanol and stored in 70% ethanol at -20^{o}C prior to RNA FISH.

XEN cells were derived as previously described (Kalantry et al., 2006). Briefly, individual embryos were plated onto irradiated mouse embryonic fibroblasts (MEF) in wells of a 4-well tissue culture dish with 750 µL of XEN cell derivation media (MEMα, 50 µg/ml penicillin/streptomycin (Life Technologies, # 15070), 20% ES qualified FBS (Life Technologies, #10439), 1 mM sodium pyruvate, 100 µM β-Mercaptoethanol, 2 mM L-glutamine, 100 µM nonessential amino acids (GIBCO, #11140), 1000 units/mL Leukemia Inhibitory Factor (LIF, Millipore # ESG1107)). Following 6-8 days of growth, blastocyst outgrowths were dissociated with 0.05% trypsin (Life Technologies, #25300). Dissociated cells were plated into individual wells of a 96-well dish containing MEFs and cultured to confluency. The cells were then split into a single well of a 4-well dish containing MEFs. After confluency, the cells were trypsinized and plated into a gelatinized well of a 6-well dish in XEN growth media (MEMα, 20% ES-FBS, 1 mM sodium pyruvate, 100 µM β-Mercaptoethanol, 2 mM L-glutamine, 100 µM nonessential amino acids). All cells in culture were grown at 37°C with 5% CO_2.

TS cells were derived similarly. Individual embryos were plated onto irradiated MEFs in wells of a 4-well tissue culture dish with 750 µL of TS cell derivation media (RPMI (0 µg/mL pen/strep), 20% ES qualified FBS, 1 mM Sodium Pyruvate, 100 µM β-Mercaptoethanol, 2 mM L-Glutamine, 37.5 ng/mL FGF4, 1.5 µg/mL Heparin). Following 4-5 days of growth, blastocyst outgrowths were dissociated with 0.05% trypsin. Dissociated cells were plated into individual wells of a 96-well dish containing MEFs and cultured to confluency. The cells were then split into a single well of a 4-well dish containing MEFs. After confluency, the cells were trypsinized and plated onto MEFs in a 6-well dish in TS growth media (RPMI, 20% ES FBS, 1 mM Sodium

Pyruvate, 100 μM β-Mercaptoethanol, 2 mM L-Glutamine, 25 ng/mL FGF4, 1.0 μg/mL Heparin). All cells in culture were grown at 37°C with 5% CO_2.

Often while deriving TS cells, XEN cells are incidentally derived. To separate TS and XEN cells growing in the same wells, TS colonies can be picked under a microscope using a P20 set to 3 μL. Picked colonies are then dissociated in trypsin and plated down in TS growth media. Cells are grown to confluency and split as described above. This process is repeated until no XEN cells are present.

DNA Lysate Collection

Cells were lysed using 0.05% trypsin and spun down at 500 rcf (5 minutes) at room temperature. Pellets were then resuspended in 15-20 μL of a DNA lysis buffer (50 mM KCl, 10 mM Tris-Cl pH 8.3, 2.5 mM MgCl2, 0.1 mg/mL gelatin, 0.45% NP-40, 0.45% Tween-20) and proteinase K mixture made at a 50:1 ratio and left in a 50°C water bath overnight. After sitting overnight, samples were heated at 90°C for 5-10 minutes before being stored at 4°C for genotyping.

Polymerase Chain Reaction (PCR) and Gel Electrophoresis

Polymerase Chain Reactions (PCRs) were used to genotype and sex cell lines, and to validate *Kdm5c* deletions in Tamoxifen-treated cells. 1 μL of extracted DNA was mixed with 24 μL of master mix solution (Klenthern Buffer (10x: 670mM Tris HCl, pH 9.1, 160mM (NH4)2SO4, 35mM MgCl2, 1.5mg/ml BSA), dNTPs (Alkali Scientific Cat.# C761), forward primers, reverse primers (Table 1), RadiantTaq (Alkali Scientific Cat# C109)).

RNA Fluorescent in Situ Hybridization (FISH) Probe

RNA FISH probes were labeled using the Bioprime Labeling kit (Invitrogen Cat.# 18094-011). Xist RNA accumulation was detected by FITC-dUTP labeled probe while Atrx RNA was detected by Cy3-dCTP labeled probe.

RNA FISH was carried out essentially as described previously (Kalantry et al., 2006).

Cells were split onto gelatinized glass coverslips and treated with either (Z)-4-Hydroxytamoxifen (Tamoxifen, PeproTech Cat.# 6800637) or molecular grade Ethanol at a concentration of 1.25 μM, and permeabilized after 24 or 48 hours. To permeablize, cells were incubated at room temperature for 20-30 seconds in cytoskeletal buffer 30 (CSK: 100 mM NaCl, 300 mM sucrose, 3 mM MgCl2, 10 mM PIPES pH 6.8), then for 20-30 seconds in CSK containing 0.4% Triton X-100, then again for 20-30 seconds in CSK. Cells were then fixed for 10 minutes in 4% paraformaldehyde, and stored at -20˚C in 70% ethanol or processed directly for RNA FISH.

For RNA FISH, cells underwent sequential incubations in 70% (5 min), 85%, 95% and 100% (2 min each) ethanol. Following this, coverslips were air-dried for 10 min, hybridized in a dsDNA probe labeled via random priming, and incubated overnight at 37˚C in a humid chamber. After incubation, coverslips were removed from the humid chamber and washed successively in 50% formamide/2X SSC buffer and 2X SSC buffer three times each for seven minutes and incubated at 39˚C. For the final 2X SSC wash, 5μL of 1:500 DAPI was added per 2mL of buffer. Coverslips were then rinsed

once in 1X SSC buffer to remove excess DAPI from the wells, before undergoing two successive washes in 1X SSC buffer under the same conditions. After the final incubation period, coverslips were mounted using Vectashield.

Microscopy

Images of all stained samples were captured using a Nikon Eclipse TiE inverted microscope with a Photometrics CCD camera. The images were analyzed after deconvolution using NIS-Elements software (version 5.20.02, Build 1453). All images were processed uniformly.

RNA Extraction

After 24, 48, or 72 hours of Tamoxifen or Ethanol treatment, cells were dissociated with 0.05% trypsin and spun down for 5 minutes at 1500 rpm. A vacuum apparatus was then used to remove the supernatant, the pellet was resuspended in 1 mL of Trizol reagent (Invitrogen Cat.# 15596-018) and stored at -80◦C for extraction. Total RNA was isolated from cells using a phenol-chloroform extraction. Briefly, 0.2mL of chloroform was added to a sample per 1mL of Trizol reagent used. Samples were mixed vigorously and left to incubate at room temperature for 2-3 minutes. Samples were then centrifuged at 12,000 rcf at 4◦C (15 minutes). After centrifugation the RNA containing aqueous phase was transferred to another tube and 0.5mL of isopropyl alcohol was added per 1mL of Trizol reagent used for initial homogenization. After incubating for 20 minutes, the samples were again centrifuged (10 minutes) to pellet the precipitated

RNA. If no RNA pellet was visible after this step, samples could be stored at -80◦C overnight to increase the amount of extracted RNA.

A vacuum apparatus was then used to remove the supernatant and the pellet was washed in 1mL of 75% ethanol. The sample was centrifuged at 7,500 rcf at 4◦C (5 minutes) and this process was repeated once. The supernatant was removed and the sample placed in the SpeedVac vacuum centrifuge for 5 minutes to dry completely. The RNA pellet was then resuspended in RNase-free water and its concentration and purity measured using a nanodrop.

RT-qPCR and PCR primers

RT-PCR was performed using the Luna Universal One-Step RT-qPCR kit (New England Biolabs) using total RNA.

Primer	Sequence	Use
qRTSmcxF	TTTGGCAGCGGTTTCCCTGTCAGT	RT-qPCR
qRTSmcxR	AAGACCATTCCCACATACAGCC	RT-qPCR
Xist1_RTqPCR F	CTCCCAGCATTACTGAGAAATG	RT-qPCR
Xist2_RTqPCR R	CCAGGCAATCCTTCTTCTTGAG	RT-qPCR
qRTtbpF	TTCAGAGGATGCTCTAGGGAAGA	RT-qPCR
qRTtbpR	CTGTGGAGTAAGTCCTGTGCC	RT-qPCR
Fabpi-SF	TGGACAGAACTGGACCTCTGCTTTCCTA	PCR
Fabpi-SR	TAGAGCTTTGCCACATCACAGGTCATTC	PCR
SmcxF2	TGGGTTTGAGGGATACTTTAGG	PCR
SmcxF5	CAGGTGGCTTACTGTGACATTGATG	PCR

SmcxR1+-	GGTTCTCAACACTCACATAGTG	PCR
WUStL-Cre-F	GCATTACCGGTCGATGCAACGAGTGATGAG	PCR
WUStL-Cre-R	GAGTGAACGAACCTGGTCGAAATCAGTGCG	PCR
XX-XY-F	CCGCTGCCAAATTCTTTGG	PCR
XX-XY-R	TGAAGCTTTTGGCTTTGAGC	PCR

Table 1: List of primers used for RT-qPCR and PCR

Acknowledgments

I would like to acknowledge my mentor Dr. Sundeep Kalantry for providing me the opportunity to work in his lab for the last four years. The research I have conducted for the Kalantry lab has been invaluable in shaping my future career path. It has deepened my understanding of the scientific process and developed my skills as an effective scientist and researcher. Dr. Kalantry has been an exceptional mentor, providing insightful and critical feedback on my experimental progress. I would also like to thank Clair Harris who has worked with and advised me on a day to day basis while also being a constant supportive presence in my life. Clair taught me many of the skills and scientific background necessary to perform these experiments, and additionally helped me maintain cell lines and conduct experiments when I could not fit them into my busy schedule. I would like to thank other members of the Kalantry lab who were willing to answer any questions I may have, and who created a supportive environment that I felt a part of. Finally I would like to thank Professor Michal Zochowski who co-sponsored this research. Without his help I would not have been able to write this thesis.

References

Aeby, E. et al. Decapping enzyme 1A breaks X-chromosome symmetry by controlling Tsix elongation and RNA turnover. *Nat. Cell Biol*. 22, 1116–1129 (2020).

Agulnik, A. I. et al. A novel X gene with a widely transcribed Y-linked homologue escapes X-inactivation in mouse and human. *Hum. Mol. Genet.* 3, 879–884 (1994).

Augui, S. et al. Sensing X chromosome pairs before X inactivation via a novel X-pairing region of the Xic. *Science* 318, 1632–1636 (2007).

Augui, S., Nora, E. P. & Heard, E. Regulation of X-chromosome inactivation by the X-inactivation centre. *Nat. Rev. Genet.* 12, 429–442 (2011).

Avner, P., Heard, E. X-chromosome inactivation: counting, choice and initiation. *Nat Rev Genet 2,* 59–67 *(2001)*.

Bacher, C. P. et al. Transient colocalization of X-inactivation centres accompanies the initiation of X inactivation. *Nat. Cell Biol.* 8, 293–299 (2006).

Barakat, T. S. et al. The trans-activator RNF12 and cis-acting elements effectuate X chromosome inactivation independent of X-pairing. *Mol. Cell* 53, 965–978 (2014).

Bellott, D. W. & Page, D. C. Reconstructing the evolution of vertebrate sex chromosomes. *Cold Spring Harb. Symp. Quant. Biol.* 74, 345–353 (2009).

Bellott, D. W. et al. Mammalian Y chromosomes retain widely expressed dosage-sensitive regulators. *Nature* 508, 494–499 (2014).

Berletch, J. B., Yang, F., Xu, J., Carrel, L. & Disteche, C. M. Genes that escape from X inactivation. *Hum. Genet.* 130, 237–245 (2011).

Boggs, B. A. et al. Differentially methylated forms of histone H3 show unique association patterns with inactive human X chromosomes. *Nat. Genet.* 30, 73–76 (2002).

Brawand, D. et al. The evolution of gene expression levels in mammalian organs. *Nature* 478, 343–348 (2011).

Brockdorff N, Turner BM. Dosage compensation in mammals. *Cold Spring Harb Perspect Biol.* Mar 2;7(3):a019406 (2015).

Brons, I. G. et al. Derivation of pluripotent epiblast stem cells from mammalian embryos. *Nature* 448, 191–195 (2007).

Brown, C. J. et al. The human XIST gene: analysis of a 17 kb inactive X-specific RNA that contains conserved repeats and is highly localized within the nucleus. *Cell* 71, 527–542 (1992).

Bryja, V., Bonilla, S. & Arenas, E. Derivation of mouse embryonic stem cells. *Nat. Protoc.* 1, 2082–2087 (2006).

Buecker, C. et al. Reorganization of enhancer patterns in transition from naive to primed pluripotency. *Cell Stem Cell* 14, 838–853 (2014).

Calabrese, J. M. et al. Site-specific silencing of regulatory elements as a mechanism of X inactivation. Cell 151, 951–963 (2012).

Carrel, L., Hunt, P. A. & Willard, H. F. Tissue and lineage-specific variation in inactive X chromosome expression of the murine Smcx gene. *Hum. Mol. Genet*. 5, 1361–1366 (1996).

Chureau, C. et al. Ftx is a non-coding RNA which affects Xist expression and chromatin structure within the X-inactivation center region. *Hum. Mol. Genet.* 20, 705–718 (2011).

Chu, C. et al. Systematic discovery of xist RNA binding proteins. *Cell* 161, 404–416 (2015).

Cloutier, M., Harris, C., Gayen, S., Maclary, E. & Kalantry, S. Experimental analysis of imprinted mouse X-chromosome inactivation. *Methods Mol. Biol.* 1861, 177–203 (2018).

Clemson, C. M., McNeil, J. A., Willard, H. F. & Lawrence, J. B. XIST RNA paints the inactive X chromosome at interphase: evidence for a novel RNA involved in nuclear/chromosome structure. *J. Cell Biol.* 132, 259–275 (1996).

Cortez, D. et al. Origins and functional evolution of Y chromosomes across mammals. *Nature* 508, 488–493 (2014).

Del Rosario, B. C. et al. Genetic intersection of Tsix and Hedgehog signaling during the initiation of X-chromosome inactivation. *Dev. Cell* 43, 359–371 e6 (2017).

Dobin, A. et al. STAR: ultrafast universal RNA-seq aligner. *Bioinformatics* 29, 15–21 (2013).

Donnelly, L., Harris, C., & Kalantry, S. (2014). Evidence of Polycomb-independent Catalysis of Histone H3 Lysine 27 Trimethylation, *University of Michigan Science in Cellular and Molecular Biology.*

Dossin, F. et al. SPEN integrates transcriptional and epigenetic control of X-inactivation. *Nature* 578, 455–460 (2020).

Duret, L., Chureau, C., Samain, S., Weissenbach, J. & Avner, P. The Xist RNA gene evolved in eutherians by pseudogenization of a protein-coding gene. *Science* 312, 1653–1655 (2006).

Egan, B. et al. An alternative approach to ChIP-Seq normalization enables detection of genome-wide changes in histone H3 lysine 27 trimethylation upon EZH2 inhibition. *PLoS ONE 11*, e0166438 (2016).

Furlan, G. et al. The Ftx noncoding locus controls X chromosome inactivation independently of its RNA products. *Mol. Cell* 70, 462–472.e8 (2018).

Gayen, S., Maclary, E., Buttigieg, E., Hinten, M. & Kalantry, S. A primary role for the Tsix lncRNA in maintaining random X-chromosome inactivation. *Cell Rep*. 11, 1251–1265 (2015).

Gayen, S., Maclary, E., Hinten, M. & Kalantry, S. Sex-specific silencing of X-linked genes by Xist RNA. *Proc. Natl Acad. Sci. USA* 113, E309–E318 (2016).

Gjaltema, R. A. F. et al. Distal and proximal cis-regulatory elements sense X chromosome dosage and developmental state at the Xist locus. *Mol. Cell* 82, 190–208 (2021).

Gontan, C. et al. RNF12 initiates X-chromosome inactivation by targeting REX1 for degradation. *Nature* 485, 386–390 (2012).

Grant, J. et al. Rsx is a metatherian RNA with Xist-like properties in X-chromosome inactivation. *Nature* 487, 254–258 (2012).

Graves, J. A. Evolution of vertebrate sex chromosomes and dosage compensation. *Nat. Rev. Genet.* 17, 33–46 (2016).

Hadjantonakis, A. K., Gertsenstein, M., Ikawa, M., Okabe, M. & Nagy, A.Non-invasive sexing of preimplantation stage mammalian embryos. *Nat. Genet*. 19, 220–222 (1998).

Harris, C. et al. Conversion of random X-inactivation to imprinted X-inactivation by maternal PRC2. *eLife* 8, e44258 (2019).

Hayashi, S., Lewis, P., Pevny, L. & McMahon, A. P. Efficient gene modulation in mouse epiblast using a Sox2Cre transgenic mouse strain. *Gene Expr.* Patterns 2, 93–97 (2002).

Hayashi, K., Ohta, H., Kurimoto, K., Aramaki, S. & Saitou, M. Reconstitution of the mouse germ cell specification pathway in culture by pluripotent stem cells. *Cell* 146, 519–532 (2011).

Heintzman, N. D. et al. Histone modifications at human enhancers reflect global cell-type-specific gene expression. *Nature* 459, 108–112 (2009).
Hinten, M., Maclary, E., Gayen, S., Harris, C. & Kalantry, S. Visualizing long noncoding RNAs on chromatin. *Methods Mol. Biol*. 1402, 147–164 (2016).

Horton, J. R. et al. Characterization of a linked Jumonji domain of the KDM5/ JARID1 family of histone H3 lysine 4 demethylases. *J. Biol. Chem.* 291, 2631–2646 (2016).

Iwase, S. et al. The X-linked mental retardation gene SMCX/JARID1C defines a family of histone H3 lysine 4 demethylases. *Cell* 128, 1077–1088 (2007).

Iwase, S. et al. A mouse model of X-linked intellectual disability associated with impaired removal of histone methylation. *Cell Rep*. 14, 1000–1009 (2016).

Jachowicz, J. W. et al. Xist spatially amplifies SHARP/SPEN recruitment to balance chromosome-wide silencing and specificity to the X chromosome. *Nat. Struct. Mol. Biol.* 29, 239–249 (2022).

Jegalian, K. & Page, D. C. A proposed path by which genes common to mammalian X and Y chromosomes evolve to become X inactivated. *Nature* 394, 776–780 (1998).

Jonkers, I. et al. RNF12 is an X-Encoded dose-dependent activator of X chromosome inactivation. *Cell* 139, 999–1011 (2009).

Kalantry, S. & Magnuson, T. The Polycomb group protein EED is dispensable for the initiation of random X-chromosome inactivation. PLoS Genet. 2, e66 (2006).

Kalantry, S., et al. The Polycomb Group protein EED protects the inactive X-chromosome from differentiation-induced reactivation. *Nature Cell Biology*, *8*(2), 195–202 (2006).

Kalantry, S., Purushothaman, S., Bowen, R. B., Starmer, J. & Magnuson, T. Evidence of Xist RNA-independent initiation of mouse imprinted X-chromosome inactivation. *Nature* 460, 647–651 (2009).

Kalantry, S. Recent advances in X-chromosome inactivation. *J. Cell Physiol.* 226, 1714–1718 (2011).

Kashimada, K. & Koopman, P. Sry: the master switch in mammalian sex determination. *Development* 137, 3921–3930 (2010).

Korczynska, M. et al. Docking and linking of fragments to discover Jumonji histone demethylase inhibitors. *J. Med Chem*. 59, 1580–1598 (2016).

Lahn, B. T. & Page, D. C. Four evolutionary strata on the human X chromosome. *Science* 286, 964–967 (1999).

Langmead, B., Trapnell, C., Pop, M. & Salzberg, S. L. Ultrafast and memory-efficient alignment of short DNA sequences to the human genome. *Genome Biol*. 10, R25 (2009).

Lewandoski, M., Wassarman, K. M. & Martin, G. R. Zp3-cre, a transgenic mouse line for the activation or inactivation of loxP-flanked target genes specifically in the female germ line. *Curr. Biol*. 7, 148–151 (1997).

Lyon, M. F. Gene action in the X-chromosome of the mouse (Mus musculus L.). *Nature* 190, 372–373 (1961).

Maclary, E., Hinten, M., Harris, C. & Kalantry, S. Long noncoding RNAs in the X-inactivation center. Chromosome Res 21, 601–614 (2013).

Maclary, E. et al. Differentiation-dependent requirement of Tsix long non-coding RNA in imprinted X-chromosome inactivation. *Nat. Commun*. 5, 4209 (2014).

Madeira, F. et al. The EMBL-EBI search and sequence analysis tools APIs in 2019. *Nucleic Acids Res*. 47, W636–W641 (2019).

Mahadevaiah, S. K. et al. Mouse homologues of the human AZF candidate gene RBM are expressed in spermatogonia and spermatids, and map to a Y chromosome deletion interval associated with a high incidence of sperm abnormalities. *Hum. Mol. Genet.* 7, 715–727 (1998).

Marahrens, Y., et al. Xist-deficient mice are defective in dosage compensation but not spermatogenesis. *Genes & development*, *11*(2), 156–166. (1997)

Marchler-Bauer, A. et al. CDD: NCBI's conserved domain database. *Nucleic Acids Res.* 43, D222–D226 (2015).

Masui, S. et al. Rex1/Zfp42 is dispensable for pluripotency in mouse ES cells. *BMC Dev. Biol*. 8, 45 (2008).

McHugh, C. A. et al. The Xist lncRNA interacts directly with SHARP to silence transcription through HDAC3. *Nature* 521, 232–236 (2015).

McMahon, A., Fosten, M. & Monk, M. X-chromosome inactivation mosaicism in the three germ layers and the germ line of the mouse embryo. *J. Embryol. Exp. Morphol.* 74, 207–220 (1983).

Minajigi, A. et al. Chromosomes. A comprehensive Xist interactome reveals cohesin repulsion and an RNA-directed chromosome conformation. *Science* 349, aab2276 (2015).

Moindrot, B. et al. A Pooled shRNA Screen Identifies Rbm15, Spen, and Wtap as Factors Required for Xist RNA-Mediated Silencing. *Cell Rep.* 12, 562–572 (2015).

Monfort, A. et al. Identification of Spen as a crucial factor for Xist function through forward genetic screening in haploid embryonic stem cells. *Cell Rep.* 12, 554–561 (2015).

Mutzel, V. et al. A symmetric toggle switch explains the onset of random X inactivation in different mammals. Nat. St*ruct. Mol. Biol.* 26, 350–360 (2019).

Ng, K., et al. *xist* and the order of silencing. *EMBO Reports*, *8*(1), 34–39 (2007).

Ohno, S. In Sex Chromosomes and Sex-linked Genes, x, 192 (*Springer-Verlag,* 1967).

Orlando, D. A. et al. Quantitative ChIP-Seq normalization reveals global modulation of the epigenome. *Cell Rep*. 9, 1163–1170 (2014).

Panning, B., Dausman, J., & Jaenisch, R. X chromosome inactivation is mediated by Xist RNA stabilization. *Cell*, *90*(5), 907–916 (1997).

Penny, G. D., Kay, G. F., Sheardown, S. A., Rastan, S. & Brockdorff, N Requirement for Xist in X chromosome inactivation. *Nature* 379, 131–137 (1996).

Pettersson, U. Faculty opinions recommendation of epigenetic dynamics of imprinted x inactivation during early mouse development. *Faculty Opinions – Post-Publication Peer Review of the Biomedical Literature*. (2004).

Pollex, T. & Heard, E. Nuclear positioning and pairing of X-chromosome inactivation centers are not primary determinants during initiation of random X-inactivation. *Nat. Genet.* 51, 285–295 (2019).

Posynick, B. J. & Brown, C. J. Escape from X-chromosome inactivation: an evolutionary perspective. Front. *Cell Dev. Biol.* 7, 241 (2019).

Przeworski, M. Faculty opinions recommendation of the Xist RNA gene evolved in Eutherians by pseudogenization of a protein-coding gene. *Faculty Opinions – Post-Publication Peer Review of the Biomedical Literature*. (2006).

Rada-Iglesias, A. Is H3K4me1 at enhancers correlative or causative? *Nature Genetics*, *50*(1), 4–5 (2017).

Rada-Iglesias, A. et al. A unique chromatin signature uncovers early developmental enhancers in humans. *Nature* 470, 279–283 (2011).

Rastan, S. & Robertson, E. J. X-chromosome deletions in embryo-derived (EK) cell lines associated with lack of X-chromosome inactivation. *J. Embryol.* Exp. Morphol. 90, 379–388 (1985).

Rastan, S. Primary non-random X-inactivation caused by controlling elements in the mouse demonstrated at the cellular level. Genet Res. 40, 139–147 (1982). 25. Marahrens, Y. X-inactivation by chromosomal pairing events. *Genes Dev.* 13, 2624–2632 (1999).

Rens, W., Wallduck, M. S., Lovell, F. L., Ferguson-Smith, M. A. & Ferguson-Smith, A. C. Epigenetic modifications on X chromosomes in marsupial and monotreme mammals and implications for evolution of dosage compensation. *Proc. Natl Acad. Sci. USA* 107, 17657–17662 (2010).

Robert-Finestra, T. et al. SPEN is required for Xist upregulation during initiation of X chromosome inactivation. *Nat. Commun*. 12, 7000 (2021).

Sado, T., Wang, Z., Sasaki, H. & Li, E. Regulation of imprinted X-chromosome inactivation in mice by Tsix. *Development* 128, 1275–1286 (2001)

Samanta, M., et al. Activation of Xist by an evolutionarily conserved function of KDM5C Demethylase. *Nature Communications*, *13*(1) (2022).

Samanta, M. & Kalantry, S. Generating primed pluripotent epiblast stem cells: a methodology chapter. *Curr. Top. Dev. Biol.* 138, 139–174 (2020).

Sarkar, M. K. et al. An Xist-activating antisense RNA required for X-chromosome inactivation. *Nat. Commun.* 6, 8564 (2015).

Sheardown, S., Norris, D., Fisher, A. & Brockdorff, N. The mouse Smcx gene exhibits developmental and tissue specific variation in degree of escape from X inactivation. *Hum. Mol. Genet*. 5, 1355–1360 (1996).

Shin, J. et al. Maternal Rnf12/RLIM is required for imprinted X-chromosome inactivation in mice. *Nature* 467, 977–981 (2010).

Shin, J. et al. RLIM is dispensable for X-chromosome inactivation in the mouse embryonic epiblast. *Nature* 511, 86–89 (2014).

Sprague, D. et al. Nonlinear sequence similarity between the Xist and Rsx long noncoding RNAs suggests shared functions of tandem repeat domains. *RNA* 25, 1004–1019 (2019).

Sun, B. K., Deaton, A. M. & Lee, J. T. A transient heterochromatic state in Xist preempts X inactivation choice without RNA stabilization. *Mol. Cell* 21, 617–628 (2006).

Tahiliani, M. et al. The histone H3K4 demethylase SMCX links REST target genes to X-linked mental retardation. *Nature* 447, 601–605 (2007).

Takada, T. et al. The ancestor of extant Japanese fancy mice contributed to the mosaic genomes of classical inbred strains. *Genome Res*. 23, 1329–1338 (2013).

Takagi, N., Wake, N. & Sasaki, M. Cytologic evidence for preferential inactivation of the paternally derived X chromosome in XX mouse blastocysts. *Cytogenet Cell Genet.* 20, 240–248 (1978).

Tesar, P. J. et al. New cell lines from mouse epiblast share defining features with human embryonic stem cells. *Nature* 448, 196–199 (2007).

Tian, D., Sun, S. & Lee, J. T. The long noncoding RNA, Jpx, is a molecular switch for X chromosome inactivation. *Cell* 143, 390–403 (2010).

UniProt, C. The universal protein resource (UniProt) 2009. *Nucleic Acids Res.* 37, D169-D174 (2009).

Wang, F. et al. Rlim-dependent and -independent pathways for X chromosome inactivation in female ESCs. *Cell Rep.* 21, 3691–3699 (2017).

Wang, X., Douglas, K. C., Vandeberg, J. L., Clark, A. G. & Samollow, P. B. Chromosome-wide profiling of X-chromosome inactivation and epigenetic states in fetal brain and placenta of the opossum, Monodelphis domestica. *Genome Res.* 24, 70–83 (2014).

Warren, W. C. et al. Genome analysis of the platypus reveals unique signatures of evolution. *Nature* 453, 175–183 (2008).

Wu, J. et al. Isolation and characterization of XE169, a novel human gene that escapes X-inactivation. *Hum. Mol. Genet.* 3, 153–160 (1994).

Xu, N., Tsai, C. L. & Lee, J. T. Transient homologous chromosome pairing marks the onset of X inactivation. *Science* 311, 1149–1152 (2006).

Yachdav, G. et al. MSAViewer: interactive JavaScript visualization of multiple sequence alignments. *Bioinformatics* 32, 3501–3503 (2016).

Zhang, Y. et al. Model-based analysis of ChIP-Seq (MACS). *Genome Biol.* 9, R137 (2008).

Zhou, Y. et al. Platypus and echidna genomes reveal mammalian biology and evolution. *Nature* 592, 756–762 (2021).

Zylicz, J. J. et al. The implication of early chromatin changes in X chromosome inactivation. *Cell* 176, 182–197.e23 (2019).